American Mineralogist, Volume 90, pages 266–270, 2005

LETTER

Pressure dependence of the OH-stretching mode in F-rich natural topaz and topaz-OH

K. KOMATSU,[1,2,*] H. KAGI,[2] T. OKADA,[2,†] T. KURIBAYASHI,[1] J.B. PARISE,[3] AND Y. KUDOH[1]

[1]Institute of Mineralogy, Petrology and Economic Geology, Graduate School of Science, Tohoku University, Sendai 980-8578, Japan
[2]Laboratory for Earthquake Chemistry, Graduate School of Science, The University of Tokyo, Tokyo 113-0033, Japan
[3]Departments of Geosciences and Chemistry, SUNY at Stony Brook, Stony Brook, New York 11794-2100, U.S.A.

ABSTRACT

OH stretching vibration modes for F-rich natural topaz (F-topaz) and for fully hydrated topaz (topaz-OH) synthesized at high pressure, were observed using IR and Raman spectroscopies at pressures up to 30.4 GPa and 17.3 GPa, respectively. In F-topaz, the pressure derivative of the frequency of the OH stretching band observed at 3650 cm^{-1} at ambient pressure was 0.91(3) cm^{-1}/GPa, which was consistent with the value recently reported by Bradbury and Williams (2003). On the other hand, in topaz-OH, the pressure derivatives of the bands initially at 3599 and 3522 cm^{-1} were –5.2(2) and –2.56(6) cm^{-1}/GPa, respectively. This contrasting behavior between the two forms of topaz at high pressures suggests that the OH substitution for F in topaz affects the hydrogen-bonding behavior under high pressure.

INTRODUCTION

Topaz [$Al_2SiO_4(OH,F)_2$] is a well-known hydrous mineral abundant in the crust. In near-surface environments, substitution of F by OH in topaz occurs within a limited range [OH/(OH + F) < ~30%] (e.g., Ribbe and Rosenberg 1971). The existence of an upper limit of OH content is rationalized in terms of the distribution of hydrogen over two closely spaced sites (e.g., Parise et al. 1980; Barton 1982). Based on an accurate determination of the structure using single crystal neutron diffraction, Parise et al. (1980) located two sites for hydrogen 1.5 Å apart (Fig. 1a). These authors noted that this structural model was inconsistent with full occupancy of both sites and so a hydrogen atom should only occupy one of the two sites, limiting the OH substitution for F to 50%. Based on subsequent energy calculations, however, Abbott (1990) suggested that the OH end-member of topaz [OH/(OH + F) = 100%] might exist because of the stabilization by hydrogen bonding.

Wunder et al. (1993) succeeded in synthesizing the OH end-member of topaz at pressures between 5.5 and 10 GPa and temperatures up to 1000 °C in the system Al_2O_3-SiO_2-H_2O. They designated this pure hydroxyl end-member as "topaz-OH." Northrup et al. (1994) determined the structure of topaz-OH from single crystal X-ray diffraction data, and showed that hydrogen atoms were distributed over two non equivalent sites (Fig. 1b). These sites (H1 and H2) in topaz-OH are statistically occupied and do not correspond to the one site found in the naturally occurring fluorine-containing topaz. Both sites in topaz-OH lie close to the mirror plane in space group *Pbnm*, but while full occupancy of the H2 site results in unreasonably short contacts of about 1.7 Å, the distance between H1 sites is approximately 2.7 Å, corresponding to about twice the van-der-Waals radius (1.2 Å) for hydrogen. At high pressures, compositions with OH/F > 0.5 clearly require occupation of at least one of the two H1 sites (Fig. 1b) in order to avoid the unfavorable contacts to the H2 sites.

It is proposed that both topaz-OH and F-rich natural topaz possess weak hydrogen bonding at ambient pressure. Belokoneva et al. (1993) identified the O1 or O2 sites as possible hydrogen bond acceptors from high-precision single-crystal X-ray diffraction data, and suggested a preference for the O-H2···O2; the O-H···O2 angle is about 139° while the O-H···O1 angle is 95°. To better understand the effects of F for OH substitution on hydrogen bonding in topaz, it is useful to compare the pressure responses of hydrogen bonds in F-topaz and topaz-OH. Wunder et al. (1999) investigated IR spectra of topaz-OH at ambient pressure and showed that the OH stretching frequencies of topaz-OH were lower than those of F-topaz, suggesting that the hydrogen bonds in topaz-OH are stronger than those in F-topaz. In this study, our attention is focused on comparing the pressure responses of the weak hydrogen bond of F-topaz to that of the stronger hydrogen bond of topaz-OH, and how the substitution of OH for F affects the behavior of hydrogen bonding under high pressure.

EXPERIMENTAL METHODS

Sample preparation

Fluorine-rich natural topaz (F-topaz) and fully hydrated synthesized topaz (topaz-OH) were investigated in this study. A colorless single crystal of natural topaz from Gilgit division, Pakistan was used as a sample of F-topaz. The chemical composition of this F-topaz was determined by electron probe micro analyzer (EPMA: JEOL, JXA-8800M) which produced a chemical formula $Al_{2.01}Si_{1.00}O_4F_{1.57}(OH)_{0.43}$; the hydroxyl component of the natural topaz was determined from the residual in the fluorine component. This sample was the same one used by Komatsu et al. (2003) for high-pressure and high-temperature single-crystal X-ray diffraction.

Topaz-OH was synthesized at high pressure and high temperature using a 2:1 mixture of $Al(OH)_3$ and SiO_2 glass powders, which provided an excess of H_2O compared to the stoichiometric composition of topaz-OH. These starting materials

* E-mail: komatsu@ganko.tohoku.ac.jp
† Present address: Department of Earth and Space Science, Graduate School of Science, Osaka University, Osaka 560-0043, Japan.

0003-004X/05/0001–266$05.00/DOI:10.2138/am.2005.1652

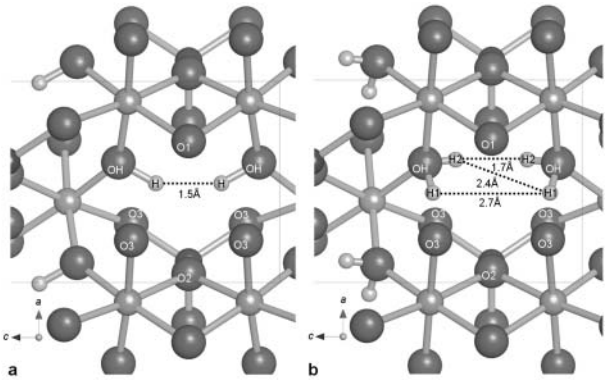

FIGURE 1. Local structures surrounding hydrogen atoms in (**a**) F-topaz and (**b**) topaz-OH. The atomic positions were determined by Belokoneva et al. (1993) and Northrup et al. (1994), respectively.

were loaded into a welded platinum capsule, which was then placed into a solid pressure medium with a graphite resistance furnace for synthesis in a Kawai-type high-pressure apparatus driven by a pair of guide blocks in a uniaxial 2000-ton press (ERI-2000) installed at the Earthquake Research Institute, University of Tokyo. Eight tungsten carbide (WC) cubic anvils having 8 mm truncation edge lengths were used. The temperature of the sample was monitored with a chromel-alumel thermocouple. The sample was held at 10 GPa and 800 °C for 18 h prior to temperature quenching followed by release of pressure. The recovered samples were confirmed as topaz-OH by powder XRD (Rigaku, MiniFlex). No impurity phase was observed within the detection limit of powder XRD.

FTIR spectra

Infrared absorption spectra of F-topaz were measured using FTIR spectrometer (Perkin Elmer, Spectra 2000) equipped with an IR microscope, a Globar light source (unpolarized), KBr beam splitter, and MCT detector operating at a spectral resolution of 4 cm^{-1}. At ambient pressure, the spectrum of air was used as a reference. A diamond anvil cell (DAC) consisting of a pair of Type Ia diamonds with 600 μm flat culets was used for high-pressure measurements up to 30.4 GPa. A thin plate of F-topaz cut parallel to (001) was placed in a gasket hole with ϕ = 150 μm in a 0.1 mm thick stainless steel (SUS301) plate with fluorinert as a fluid pressure transmitting medium. The incident light propagated between two conical angles of 45° and 72° using Cassegrainian condensing mirrors. The *c*-axis of the sample was parallel to the vertical line of the microscope. The pressure was calibrated by the ruby fluorescence method (Mao et al. 1986). At high pressure, the spectrum of fluorinert in the DAC was used as a reference spectrum. Positions and full widths at half maxima (FWHM) for peaks were determined by fitting with Lorentzian peak-shape functions. Applying this peak-fitting procedure reduces the effective spectral resolution to 0.15 cm^{-1} (Izraeli et al. 1999).

Raman spectra

The Raman spectra were obtained with a Raman microprobe consisting of a 30 cm single polychromator equipped with an optical microscope (a 20× objective lens), Ar ion laser (operating at 514.5 nm and 20 mW at the sample surface), and a CCD camera with a resolution of 1024 × 256 pixels. The Rayleigh line was removed using a holographic supernotch filter. Further details of the instrument have been described elsewhere (Kawakami et al. 2003). The Raman shift was calibrated with standard samples of naphthalene (3056.4 cm^{-1}) and brucite (3650.0 cm^{-1}). The spectral resolution was approximately 1.5 cm^{-1} per pixel. The same diamond anvil cell was used for both high-pressure IR and Raman measurements. A 4:1 mixture of methanol/ethanol was used as a fluid pressure medium. The orientation of topaz-OH in the diamond anvil cell was unconfirmed. Other experimental details on the usage of the diamond anvil cell were identical to those for FTIR measurements at high pressure. All Raman spectra were collected with an exposure time of 600 s. Peak fitting variables, fitting function and the effective spectral resolution were the same as for the FTIR measurement. Special care was taken to measure Raman spectra at the same point on the crystal with increasing pressure to minimize analytical errors induced by pressure gradients within the cell.

RESULTS AND DISCUSSION

IR and Raman spectra at ambient pressure

The IR absorption spectrum of F-topaz and the Raman spectrum of topaz-OH, both obtained at ambient conditions, are shown in Figures 2 and 3, respectively. The IR spectrum of F-topaz at ambient pressure shows a sharp band at 3650 cm^{-1} (band 1 in Fig. 2) and a weak shoulder at 3639 cm^{-1} (band 2 in Fig. 2). These frequencies agree with those reported in previous studies (Aines and Rossman 1985; Beny and Piriou 1987; Shinoda and Aikawa 1994, 1997) and were assigned to OH stretching modes. Aines and Rossman (1985) describe several "anomalous" secondary OH absorption bands that, with the exception of the absorption band at 3650 cm^{-1}, were associated

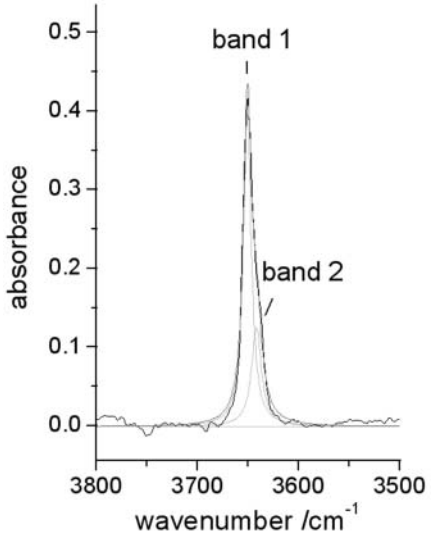

FIGURE 2. IR spectrum of F-topaz at ambient conditions.

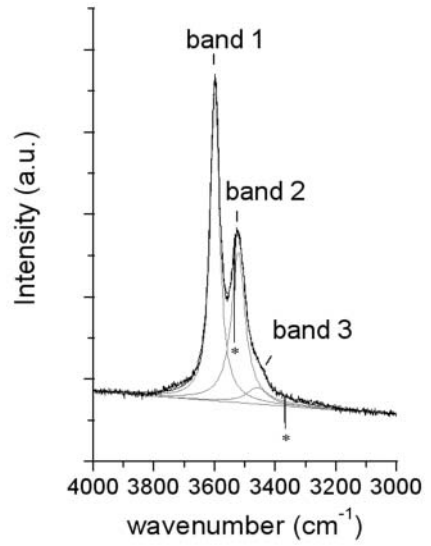

FIGURE 3. Raman spectrum of topaz-OH at ambient conditions, "*" represents noise from cosmic rays.

with structural OH defects in the 3640–3200 cm^{-1} region. The "anomalous" secondary OH absorptions were not detected in the present study.

The Raman spectrum of topaz-OH observed at ambient pressure exhibits two bands at 3599 cm^{-1} (band 1, Fig. 3) and at 3522 cm^{-1} (band 2, Fig. 3) and a weak shoulder at 3458 cm^{-1} (band 3, Fig. 3). The relative intensities of these three bands changed in individual experiments due to the orientation of the sample. Wunder et al. (1999) obtained IR spectra from topaz-OH showing bands at 3602.1, 3526.3, and 3457 cm^{-1} at ambient pressure. If the space group of topaz-OH is *Pbnm*, then the four hydrogen atoms per Bravais unit cell occupy the H1 and H2 sites at Wyckoff 8*d* sites. In this case, the IR and Raman active modes are represented as follows:

$$\Gamma_{IR} = 18\ A_g + 15\ B_{1g} + 18\ B_{2g} + 15\ B_{3g}$$
$$\Gamma_{Raman} = 17\ B_{1u} + 14\ B_{2u} + 17\ B_{3u}.$$

Three hydrogen-related modes with one OH stretching mode are included in the respective symmetry species. However, as pointed out by Northrup et al. (1994), the true symmetry of topaz-OH might be lower than *Pbnm*, at least locally. For example, if the symmetry of topaz-OH is reduced from *Pbnm* to $Pbn2_1$, the 8*d* site in *Pbnm* splits into two 4*a* sites in $Pbn2_1$. The four hydrogen atoms per Bravais unit cell now occupy either of the two 4*a* sites with site occupancies of 1.0, and therefore there are both IR and Raman active modes (32 A_1 + 32 B_1 + 32 B_2) and Raman active modes (33 A_2) with two OH stretching modes in the respective symmetry species. Although the true symmetry is unknown, it is possible that some different vibrational modes are degenerate, because the frequencies of the IR absorption bands are almost the same as those of the Raman bands.

Pressure dependences of the OH stretching modes

Representative IR spectra of F-topaz and Raman spectra of topaz-OH at high pressures are shown in Figures 4 and 5, respectively. Peak positions of the OH stretching modes of F-topaz and topaz-OH at several pressures are plotted in Figure 6. In F-topaz, the frequencies of band 1 increased linearly with increasing pressure. The frequencies of band 2 also increased with increasing pressure, but there is a slight discontinuity of the frequencies between 5.6 and 8.0 GPa. It is likely that this discontinuity is an artifact of non-hydrostatic conditions above the solidification pressure of fluorinert. This is because the FWHM of the band jumped from 12.8 cm^{-1} at 5.6 GPa to 20.2 cm^{-1} at 8.0 GPa, and the frequency correlates with the FWHM, especially in the case of the shoulder band.

The pressure derivative of the frequency of band 1 was 0.91(3) cm^{-1}/GPa. It is quite possible that the error of the pressure derivative was underestimated, because the pressure gradient within the cell did not propagate the error of the pressure derivative of the OH frequency. Except for the FWHM of this O-H stretching band, our results were roughly in agreement with those of Bradbury and Williams (2003) who reported a pressure derivative of 0.6(3) cm^{-1}/GPa. The total peak width including bands 1 and 2 at 30.4 GPa was 22.4(3) cm^{-1}, while that reported by Bradbury and Williams (2003) was approximately 80 cm^{-1}. These differences in the pressure derivatives and FWHM of the band could be related to the degree of the non-hydrostatic condition and/or the existence of a pressure gradient, since Bradbury and Williams (2003) used KBr powder as a pressure transmitting medium and used a diamond anvil with a smaller cullet size (500 μm). The small but clear positive pressure derivative of the frequency of the OH-stretching mode indicates that the hydrogen bond in F-topaz does not strengthen with increasing pressure. Bradbury and Williams (2003) also indicated that the polarizability of the O-atom weakly increased at high pressures resulting in the slightly increased hydroxyl bond strength and thus the hydroxyl-stretching frequency of F-topaz increased with compression.

In contrast to F-topaz, the frequencies of three OH stretching modes in topaz-OH decreased with increasing pressure (Fig. 5). The frequency of band 1 decreased almost linearly with compres-

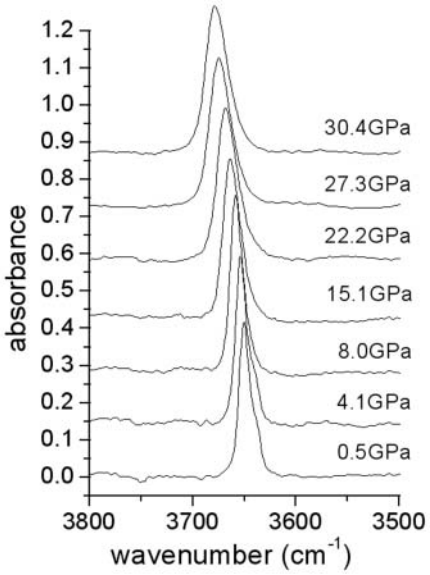

FIGURE 4. Selected IR spectra of F-topaz from ambient pressure to 30.4 GPa.

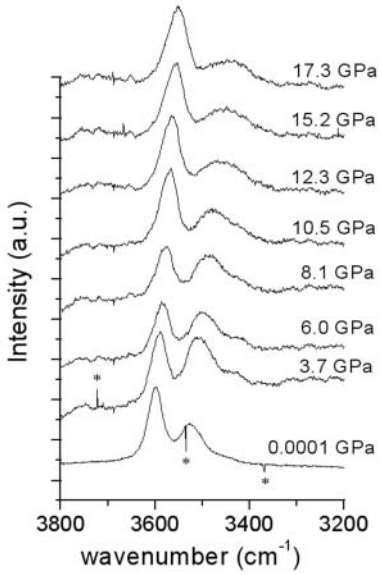

FIGURE 5. Selected Raman spectra of topaz-OH from ambient pressure to 17.3 GPa; "*" represents noise from cosmic rays.

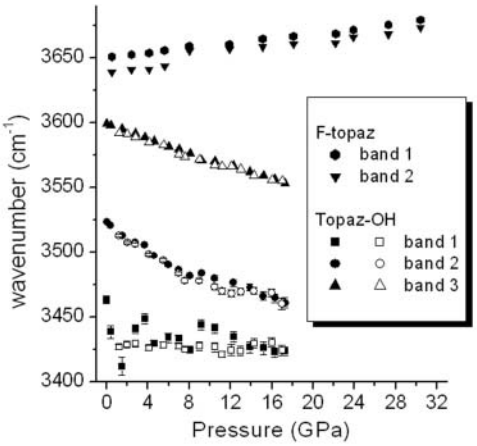

FIGURE 6. Comparison of dependencies of OH stretching modes on pressure; the filled symbols show the results on compression, and the open symbols show the results on decompression.

sion. The pressure derivative of the frequency of band 2 has a discontinuity between 8.1 and 9.2 GPa, in a manner similar to that for F-topaz, and this is probably related to the non-hydrostatic condition due to the solidification of the mixture of methanol/ethanol used as the pressure-transmitting medium. Therefore, our discussion will be restricted to the pressure-response of band 2 up to 8.1 GPa. The pressure derivative of the frequency of the band 1 was –2.56(6) cm^{-1}/GPa and that of band 2 up to 8.1 GPa was –5.2(2) cm^{-1}/GPa. The negative pressure derivatives of the OH stretching modes clearly indicate that each hydrogen bond in topaz-OH strengthens with increasing pressure.

One might question the comparison between Raman spectra of OH-topaz and IR spectra of F-topaz since there is no guarantee of the same pressure response for Raman and IR modes in this system. We therefore observed Raman spectra of F-topaz under the same experimental conditions and confirmed that the pressure derivative of the Raman shift of the OH stretching mode in F-topaz was about 0.9 cm^{-1}/GPa, the same as observed in the IR spectra. Recently, we determined the structure of F-rich natural topaz at elevated pressure (Komatsu et al. 2003). According to our results, the F···O1 and F···O2 distances at ambient pressure are 3.081(4) Å and 3.047(2) Å, respectively. These values are significantly larger than the corresponding values for topaz-OH [O(-H)···O1: 3.054 Å and O(-H)···O2: 2.961 Å] determined by Northrup et al. (1994). At 6.2 GPa, the F···O1 and F···O2 distances are 3.024(7) and 2.950(4) Å, respectively. The O(-H)···O distances in F-topaz at 6.2 GPa were close to those for topaz-OH at ambient pressure, and the O(-H)···O distances in F-topaz might keep on shortening at higher pressures. However, the hydrogen bond of F-topaz did not strengthen up to 30.4 GPa, as evidenced by the small positive shift in the pressure derivative.

Along with the O(-H)···O distance, the O-H···O angle is an important factor in determining the strength of the hydrogen bond, since it determines the degree of H*s*-O2*p* orbital overlap for the formation of the hydrogen bond, as noted by previous authors (e.g., Hofmeister et al. 1999; Bradbury and Williams 2003; Kagi et al. 2003). The O-H···O angles of topaz-OH at ambient pressure reported by Northrup et al. (1994) were in the range of 112–153° [OHa-H1-OHb: 112(4)°, OHa-H1-O2: 129(4)°, OHa-H1-O3: 152(5)°, OHb-H2-O1: 130(6)°, OHb-H2-O2: 114(6)° and OHb-H2-OHa: 153(7)°]. In F-topaz, the O-H···O angles reported by Belokoneva et al. (1993) were 95° for O-H···O1 and 139° for O-H···O2. The maximum values reported for the O-H···O angle in F-topaz and topaz-OH are 139° and 153°, respectively (Belokoneva et al. 1993; Northrup et al. 1994). If the O-H···O angles in F-topaz and in topaz-OH exhibited little change with increasing pressure, our present results and previous crystallographic data imply that there is a lower limit in the OH···O angle where the strength of the hydrogen bond shows a pressure response, and the limit of the O-H···O angle would be in the range of 139–153°. For further discussion, however, more structural information, on the pressure responses of the hydrogen bonds and the hydrogen position in topaz-OH is required.

In summary, we conclude that pressure dependences of OH stretching modes of F-topaz were positive in contrast to the negative pressure derivative found for topaz-OH. With increasing pressure, hydrogen bonds in F-topaz weaken slightly whereas those in topaz-OH strengthen. These contrasting results suggest that local structures of hydrogen bonds play an important role in controlling the pressure responses in these hydrous minerals. A combination of the present results and neutron diffraction at high pressure will be needed to obtain precise information on the H-H distance, H···O distance, and O-H···O angle under pressures.

ACKNOWLEDGMENTS

We thank A. Yasuda for access to the high-pressure facilities at the Earthquake Research Institute (ERI), University of Tokyo. Review comments from Q. Williams greatly improved the manuscript. Figure 1 was drawn with 3D visualization system VENUS developed by Dilanian and Izumi. This work is supported in part by a Grant-in-Aid for Scientific Research (13554018, 14654096, 15340190) from the Ministry of Education, Culture, Sports, Science, and Technology (MEXT). This work was also supported by a Grant-in-aid for The 21st Century COE Program for Frontiers in Fundamental Chemistry from the Ministry of Education, Culture, Sports, Science, and Technology. JBP acknowledges the support of the NSF through its EAR program.

REFERENCES CITED

Abbott, R.N. Jr. (1990) Topaz: Energy calculations bearing on the location of hydrogen. The Canadian Mineralogist, 28, 827–834.

Aines, R.D. and Rossman, G.R. (1985) The high temperature behavior of trace hydrous components in silicate minerals. American Mineralogist, 70, 1169–1179.

Barton, M.D. (1982) The thermodynamic properties of topaz solid solution and some petrological applications. American Mineralogist, 67, 956–974.

Barton, M.D., Haselton, H.T. Jr., Hemingway, B.S., Kleppa, O.J., and Robie, R.A. (1982) The thermodynamic properties of fluor-topaz. American Mineralogist, 67, 350–355.

Belokoneva, E.L., Smirnitskaya, Y.Y., and Tsirel'son, V.G. (1993) Electron density distribution in Topaz $Al_2[SiO_4](F,OH)_2$ as determination from high-precision X-ray diffraction data. Russian Journal of Inorganic Chemistry, 38-8, 1252–1256.

Beny, J.M. and Piriou, B. (1987) Vibrational spectra of single-crystal topaz. Physics and Chemistry of Minerals, 15, 148–154.

Bradbury, S.E. and Williams, Q. (2003) Contrasting bonding behavior of two hydroxyl-bearing metamorphic minerals under pressure: Clinozoisite and topaz. American Mineralogist, 88, 1460–1470.

Hofmeister, A.M., Cynn, H., Burnley, P.C., and Meade, C. (1999) Vibrational spectra of dense, hydrous magnesium silicates at high pressure: Importance of the H bond angle. American Mineralogist, 84, 454–464.

Izraeli, E.S., Harris, J.W., and Navon, O. (1999) Raman barometry of diamond formation. Earth and Planetary Science Letters, 173, 351–360.

Kagi, H., Nagai, T., Loveday, J.S., Wada, C., and Parise, J.B. (2003) Pressure-induced phase transformation of kalicinite ($KHCO_3$) at 2.8 GPa and local structural changes around hydrogen atoms. American Mineralogist, 88, 1446–1451.

Kawakami, Y., Yamamoto, J., and Kagi, H. (2003) Micro-Raman densimeter for CO_2 inclusions in mantle-derived minerals. Applied Spectroscopy, 57, 11,

1333–1339.
Komatsu, K., Kuribayashi, T., and Kudoh, Y. (2003) Effect of temperature and pressure on the crystal structure of topaz, $Al_2SiO_4(OH, F)_2$. Journal of Mineralogical and Petrological Sciences, 98-5, 167–180.
Mao, H.K., Xu, J., and Bell, P.M. (1986) Calibration of the ruby pressure gauge to 800 kbar under quasi-hydrostatic conditions. Journal of Geophysical Research, 91, 4673–4676.
Northrup, P.A., Leinenweber, K., and Parise J.P. (1994) The location of H in the high-pressure synthetic $Al_2SiO_4(OH)_2$ topaz analogue. American Mineralogist, 79, 401–404.
Parise, J.B., Cuff, C., and Moore, F.H. (1980) A neutron diffraction study of topaz: evidence for lower symmetry. Mineralogical Magazine, 43, 943–944.
Ribbe, P.H. and Gibbs, G.V. (1971) The crystal structure of topaz and its relation to physical properties. American Mineralogist, 56, 24–30.
Ribbe, P.H. and Rosenberg, P.E. (1971) Optical and X-ray determinative methods for fluorine in topaz. American Mineralogist, 57, 168–187.
Shinoda, K. and Aikawa, N. (1994) The orientation of the OH-dipole in an optically anisotropic crystal: An application to the OH-dipole in topaz. Physics and Chemistry of Minerals, 21, 24–28.
——— (1997) IR active orientation of OH bending mode in topaz. Physics and Chemistry of Minerals, 24, 551–554.
Wunder, B., Rubie, D.C., Ross, C.R. II, Medenbach, O., Seifert, F., and Schreyer, W. (1993) Synthesis, stability, and properties of $Al_2SiO_4(OH)_2$: a fully hydrated analogue of topaz. American Mineralogist, 78, 285–297.
Wunder, B., Andrut, M., and Wirth, R. (1999) High-pressure synthesis and properties of OH-rich topaz. European Journal of Mineralogy, 11, 803–813.
Yamamoto, J., Kagi, H., Kaneoka, I., Lai, Y., Prikhod'ko, V. S., and Arai, S. (2002) Fossil pressures of fluid inclusions in mantle xenoliths exhibiting rheology of mantle minerals: implications for the geobarometry of mantle minerals using micro-Raman spectroscopy. Earth and Planetary Science Letters, 198, 511–519.

Manuscript received March 20, 2004
Manuscript accepted September 16, 2004
Manuscript handled by Lee Groat